

Original paper

Geochemical characteristics of the Late Proterozoic Spitz granodiorite gneiss in the Drosendorf Unit (southern Bohemian Massif, Austria) and implications for regional tectonic interpretations

Martin LINDNER*, Fritz FINGER

*Department of Chemistry and Physics of Materials, University of Salzburg, Jakob-Haringer-Straße 2a, 5020 Salzburg, Austria;**Martin.Lindner@sbg.ac.at*** Corresponding author*

The Spitz Gneiss, located near the Danube in the southern sector of the Variscan Bohemian Massif, represents a ~13 km² large Late Proterozoic Bt ± Hbl bearing orthogneiss body in the Lower Austrian Drosendorf Unit (Moldanubian Zone). Its formation age (U–Pb zircon) has been determined previously as 614±10 Ma. Based on 21 new geochemical analyses, the Spitz Gneiss can be described as a granodioritic I-type rock (64–71 wt. % SiO₂) with medium-K composition (1.1–3.2 wt. % K₂O) and elevated Na₂O (4.1–5.6 wt. %). Compared to average granodiorite, the Spitz Gneiss is slightly depleted in Large-Ion Lithophile (LIL) elements (Rb 46–97 ppm, Cs 0.95–1.5 ppm), Sr (248–492 ppm), Nb (6–10 ppm), Th (3–10 ppm), the LREE (e.g. La 10–30 ppm), Y (6–19 ppm) and first row transitional metals (e.g. Cr 10–37 ppm). The Zr content (102–175 ppm) is close to average granodiorite. The major- and trace-element signature of the Spitz Gneiss is similar to some Late Proterozoic granodiorite suites in the Moravo–Silesian Unit (e.g. the Passendorf–Neudegg suite in the Thaya Batholith). However, granodiorites of such type and age do not occur elsewhere in the Moldanubian Zone of the Bohemian Massif. This observation fits existing tectonic models in which the Austrian Drosendorf Unit is considered allochthonous and part of the Moravo–Silesian Unit and the Avalonian Superterrane. Mineral chemistry data for amphibole, plagioclase and biotite allow an estimation of the Variscan peak regional metamorphic conditions for the Spitz Gneiss at ~700 °C and 7 kbar. Amphibole and plagioclase show hardly any signs of retrograde reequilibration, implying a fast late-Variscan exhumation. Partial chloritization of biotite indicates late fluid activity at T ~ 250 °C.

Keywords: Spitz Gneiss, Moldanubian, Bohemian Massif, Moravo–Silesian, Cadomian, Peri-Gondwana terranes

Received: 1 November, 2017; **accepted:** 30 October, 2018; **handling editor:** M. Svojtka

The online version of this article (doi: 10.3190/jgeosci.271) contains supplementary electronic material

1. Introduction

The central European Variscan fold belt hosts many remnants of Late Proterozoic to Cambrian (Cadomian) granitoids that once belonged to an Andean-type orogen along the northern Gondwana margin (Dörr et al. 2002; Linnemann et al. 2008). In the Early Paleozoic, the northern fringe of Gondwana underwent a phase of extension and fragmented into a number of terranes which drifted towards Laurentia and Baltica. These so-called peri-Gondwana terranes (Nance et al. 2008) became later incorporated into the Devonian–Carboniferous Variscan fold belt (Winchester and PACE TMR Network Team 2002; Kröner and Romer 2013) and partly underwent strong deformation and metamorphism.

The recognition and delineation of individual Peri-Gondwana terranes within the complex tectonic framework of the Variscan Orogen presents a great challenge (Tait et al. 1997; Finger et al. 2000; Franke and Źelažniewicz 2000; Friedl et al. 2000; Kalvoda et al.

2008). A potential approach for tackling this problem is a systematic collection and comparison of geochemical and geochronological data from the remnant Cadomian granitoid bodies, in the hope that they are distinctive for individual terranes.

Here we present a geochemical study for the Late Proterozoic Spitz Gneiss in the south-eastern Bohemian Massif. This orthogneiss body has been repeatedly mentioned in the literature in connection with regional tectonic issues. In particular, it has been controversially discussed whether the Spitz Gneiss and surrounding rocks (summarized as the Drosendorf Unit) are a true part of the Moldanubian core region of the Variscan Orogen or rather a tectonically emplaced slice from the Moravo–Silesian foreland plate (Frasl 1970, 1991; Matura 1976, 2003; Finger and Steyrer 1995; Finger et al. 2007b) that collided with the Moldanubian during the Variscan Orogeny (Suess 1926; Fuchs 1976; Dudek 1980).

Based on U–Pb zircon dating, Friedl et al. (2004) have constrained the magmatic formation age of the Spitz

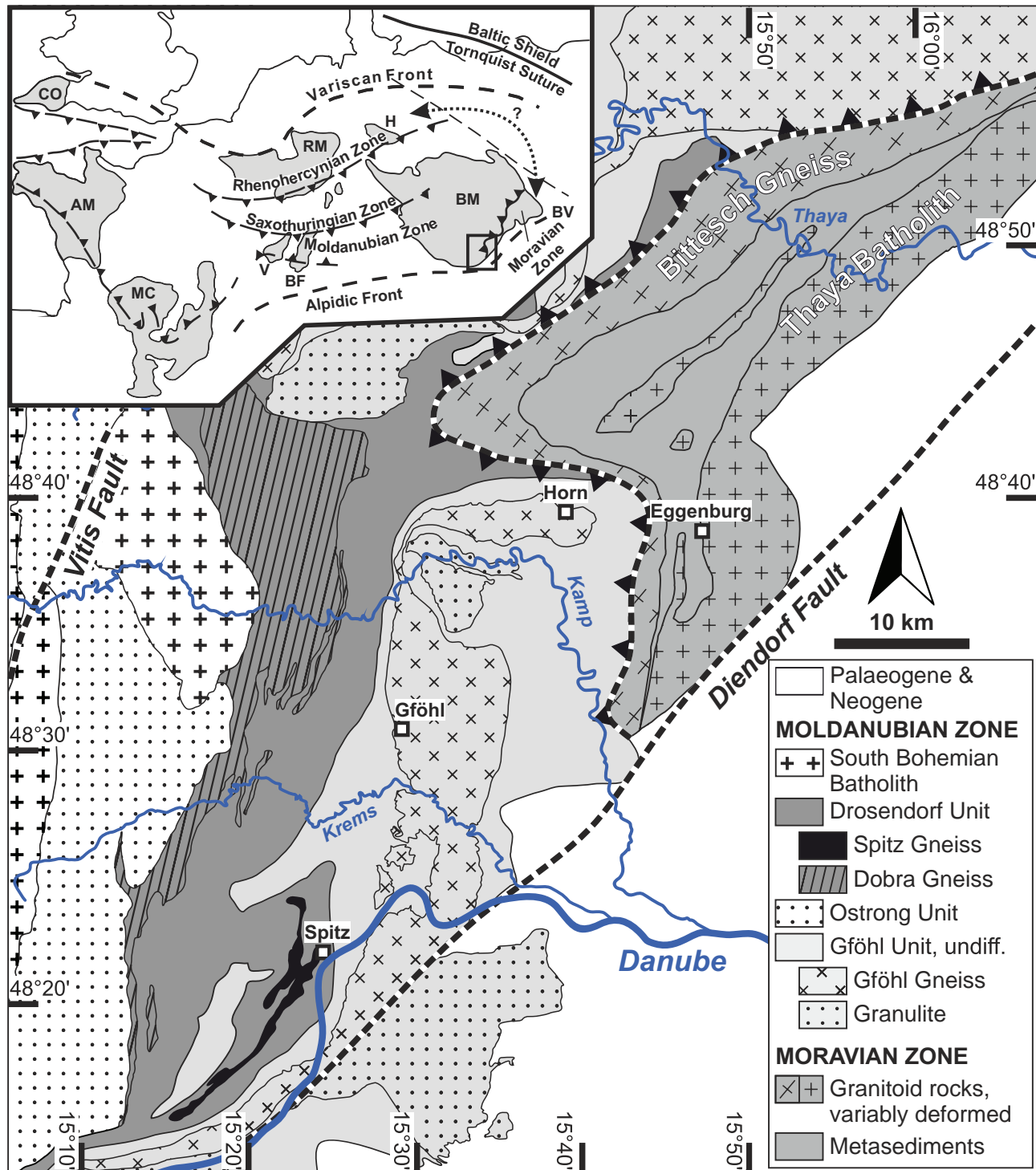


Fig. 1 Simplified geological sketch map of the study area in Lower Austria and its position in the Variscides (inset). Abbreviations: AM – Armorican Massif; BF – Black Forrest; BM – Bohemian Massif; BV – Brunovistulian (mostly covered); CO – Cornwall; H – Harz; MC – Massif Central; RM – Rhenish Massif; V – Vosges. Compiled after Fuchs and Matura (1976), Thiele (1984) and Matura (2003).

Gneiss to 614 ± 10 Ma. Conversely, the Cadomian plutonism in the Moravo–Silesian Unit was long believed to be comparably younger, i.e. ~580 Ma old (Finger et al. 2000). This age difference could be used as an argument against a Moravian affiliation of the Spitz Gneiss and the

Drosendorf Unit, respectively. However, recent age dating work in the Brno Massif has shown that the time span of Cadomian granitic activity in the Moravo–Silesian Unit was broader, covering a period from ~630 Ma to 570 Ma (Soejono et al. 2017). Comparable geochronological

dates were recently also obtained from the Thaya Batholith (Svojtka et al. 2017; W. Dörr, pers. comm.). The age of the Spitz Gneiss (614 ± 10 Ma) is, therefore, not at all in conflict with a Moravo–Silesian affiliation.

Only scarce petrographic and geochemical data have been available from the Spitz Gneiss so far (Fuchs and Matura 1976; Finger 1990), and any comparative studies with Moravo–Silesian granitoids were lacking. By introducing 21 new geochemical analyses, we are now able to comprehensively characterize the Spitz Gneiss and to compare it with Cadomian granitoids from the Moravo–Silesian Unit. Furthermore, we present a set of mineral analyses for the Spitz Gneiss, which can be used for estimating the Variscan metamorphic conditions.

2. Regional geological background

The Bohemian Massif is one of the major outcrops of the Variscan Orogen (Franke 1989, 2000; Kröner and Romer 2013). The southern half of the massif exposes the Moldanubian Zone (Kossmat 1927), the high-grade metamorphic core of the Variscan Orogen (Fig. 1). This zone represents a complex tectonic mélange (Matte et al. 1990; Franke and Želažniewicz 2000; Finger et al. 2007b; Lardeaux et al. 2014; Žák et al. 2014). In Austria, the Moldanubian has been subdivided into three tectonostratigraphic units that were juxtaposed during the Variscan Orogeny: the Gföhl, Ostrong and Drosendorf units.

The Gföhl Unit (Fig. 1) is mainly represented by felsic, variably migmatitic orthogneiss (Gföhl Gneiss), associated with paragneiss, amphibolite, felsic granulite, and locally eclogite and peridotite (Fuchs and Matura 1976; Thiele 1984; Fritz 1995; Schulmann et al. 2005; Racek et al. 2006; Hasalová et al. 2008). After a stage of subduction-related UHP and HP–HT metamorphism (O’Brien and Carswell 1993; Cooke et al. 2000; Faryad et al. 2011), the Gföhl Unit became steeply exhumed during the Variscan Orogeny (Schulmann et al. 2005).

The Ostrong Unit (Fig. 1) consists mainly of a LP–HT metamorphic monotonous series of cordierite-bearing paragneiss (Fuchs 1976; Linner 1992, 1996), likely derived from Early Paleozoic greywacke (Finger et al. 2007a; Košler et al. 2014). There are some intercalations of orthogneiss (e.g. Blaník Gneiss – Breiter et al. 2005; René and Finger 2016) and small exotic relics of eclogite which experienced severe recrystallization during the LP–HT event (O’Brien and Vrána 1995; Scott et al. 2013). It is likely that the whole Ostrong Unit is polymetamorphic (Linner 1992, 1996), but the strong Variscan LP–HT overprint has erased most of the preexisting mineral assemblages.

The Drosendorf Unit (Fig. 1) comprises a variegated series of metamorphic rocks including paragneiss, mar-

ble, quartzite, graphite schist, amphibolite, calc-silicate and orthogneiss (Fuchs and Matura 1976). All these rocks experienced Variscan MP–MT metamorphism followed by a decompression-related LP overprint (Högelsberger 1989; Petrakakis 1997). The two major orthogneiss bodies of the Drosendorf Unit are the Spitz Gneiss (614 ± 10 Ma) and the Dobra Gneiss. For the latter, a Mesoproterozoic formation age (1377 ± 10 Ma) has been postulated based on zircon dating (Gebauer and Friedl 1994). Note that we use the term Drosendorf Unit here strictly in its original sense as defined by Austrian workers, i.e., only for a distinct rock assembly in the Lower Austrian part of the Bohemian Massif.

At the end of the Variscan Orogeny, the Moldanubian Zone was intruded by the 330 to 300 Ma old granitoids of the South Bohemian Batholith (Finger et al. 1997; Gerdes et al. 2003; Breiter and Scharbert 2006; Breiter 2010; Žák et al. 2014 and references therein).

The easterly Moravian Zone (Suess 1926) was over-thrust by the Moldanubian nappes in the Carboniferous (Fritz and Neubauer 1993). It is generally interpreted as the Variscan-reactivated margin of the large Moravo–Silesian or Brunovistulian foreland plate (Dudek 1980) that forms the eastern end of the Variscides (Finger et al. 2000; Friedl et al. 2000). The Moravo–Silesian Unit exposes many Late Proterozoic granitoid rocks in the Thaya Batholith and the Brno Batholith, including granitic, granodioritic and tonalitic varieties (Finger et al. 1989, 1995; Hanzl and Melichar 1997; Leichmann and Höck 2008). Orthogneisses in the higher grade western part of the Moravian Zone (e.g., Bittesch Gneiss) have Late Proterozoic formation ages as well (Friedl et al. 2004; Soejono et al. 2017). The Moravo–Silesian granitoids are generally characterized as I-type and volcanic-arc type granites (Finger et al. 1989; Jelínek and Dudek 1993; Hanzl and Melichar 1997).

3. Methodology

3.1. Mineral chemistry

Two polished thin sections, one from a more mafic, amphibole-bearing type of Spitz Gneiss (ML 14-10), and a second from a more felsic amphibole-free type (ML 14-1B), were studied by scanning electron microscopy (SEM) and energy dispersive X-ray spectrometry (EDX) at the Department of Chemistry and Physics of Materials, University of Salzburg. The used SEM (ZEISS ULTRAPLUS) is equipped with an Oxford X-MAX 50 EDX detector plus INCA software. Mineral analyses were carried out at 15 kV and 3 nA and calibrated against natural mineral standards (quartz, garnet) and synthetic oxides.

Tab. 1 XRF analyses for the GSJ granodiorite standard JG-1a (Imai et al. 1995), including information on typical analytical errors and detection limits for individual elements

Recommended	Measured	LLD [ppm]	
SiO ₂	72.30 ± 0.51	72.40 ± 0.50	94.3
TiO ₂	0.25 ± 0.03	0.26 ± 0.01	10.0
Al ₂ O ₃	14.30 ± 0.41	14.11 ± 0.20	75.2
Fe ₂ O ₃ t	2.00 ± 0.10	1.97 ± 0.05	71.9
MgO	0.69 ± 0.07	0.72 ± 0.05	66.6
MnO	0.06 ± 0.01	0.06 ± 0.01	3.9
CaO	2.13 ± 0.08	2.15 ± 0.05	37.7
Na ₂ O	3.39 ± 0.13	3.54 ± 0.10	43.2
K ₂ O	3.96 ± 0.16	3.98 ± 0.05	28.2
P ₂ O ₅	0.08 ± 0.01	0.10 ± 0.01	24.9
H ₂ O ⁺	0.59 ± 0.13		
Sum	99.75	99.28	
Ba	470 ± 38	456 ± 10	16.5
Co	5.90 ± 1.54	5 ± 1	2.2
Cr	17.6 ± 4.4	17 ± 1	3.7
Ga	16.5 ± 0.7	15 ± 1	1.1
Gd	4.08 ± 0.63	6 ± 2	1.2
Nb	11.40 ± 0.98	13 ± 1	1.7
Ni	6.91 ± 1.90	12 ± 1	1.6
Pb	26.4 ± 2.8	22 ± 3	6.0
Rb	178 ± 10	176 ± 1	2.0
Sc	6.21 ± 0.49	6 ± 2	5.5
Sn	4.47 ± 0.56	7 ± 2	4.0
Sr	187 ± 12	178 ± 1	1.8
Th	12.8 ± 1.5	12 ± 1	2.9
V	22.7 ± 3.8	23 ± 2	6.5
Y	32.1 ± 3.8	32 ± 1	3.0
Zn	36.5 ± 2.2	39 ± 1	1.2
Zr	118 ± 13	119 ± 2	4.3

LLD = lower limit of detection

3.2. Whole-rock geochemistry

Large (2–3 kg), fresh and representative samples from 12 outcrops were collected. Weathered surfaces were removed and samples were ground to a fine powder in an agate ball mill. Twenty-one analyses were conducted by XRF methods on lithium tetraborate glass beads and pressed powder pellets using a Bruker Pioneer S4 crystal spectrometer at the Department for Chemistry and Physics of Materials, University of Salzburg. Obtained net count rates on single X-ray lines were recast into concentration data (wt. % and ppm), based on an in-house calibration routine that involves measurements of ~ 30 international geostandards (USGS and GSJ). The calibration is based on the Bruker AXS software SPECTRA^{plus} FQUANT (v1.7) and corrects absorption, fluorescence and line overlap effects. In addition, a monitor standard (GSJ Granodiorite JG-1a) was measured together with the samples. Results are given in Tab. 1 and include information on detection limits and typical analytical uncertainties for single elements. Reported errors are conservative and refer not only to the XRF counting statistics, but consider also the uncertainty of the linear fit of the calibrations. Loss on ignition (LOI) was determined gravimetrically after heating the dried powders to 1100 °C for three hours.

For four representative samples, rare earth elements, Cs, Hf, Ta, Th, and U contents were determined by ICP-MS techniques at ALS Laboratories in Laughrea, Ireland. Analyses were carried out on acid digested lithium borate fusion beads. Lower limits are between 0.01 ppm and 0.1 ppm.

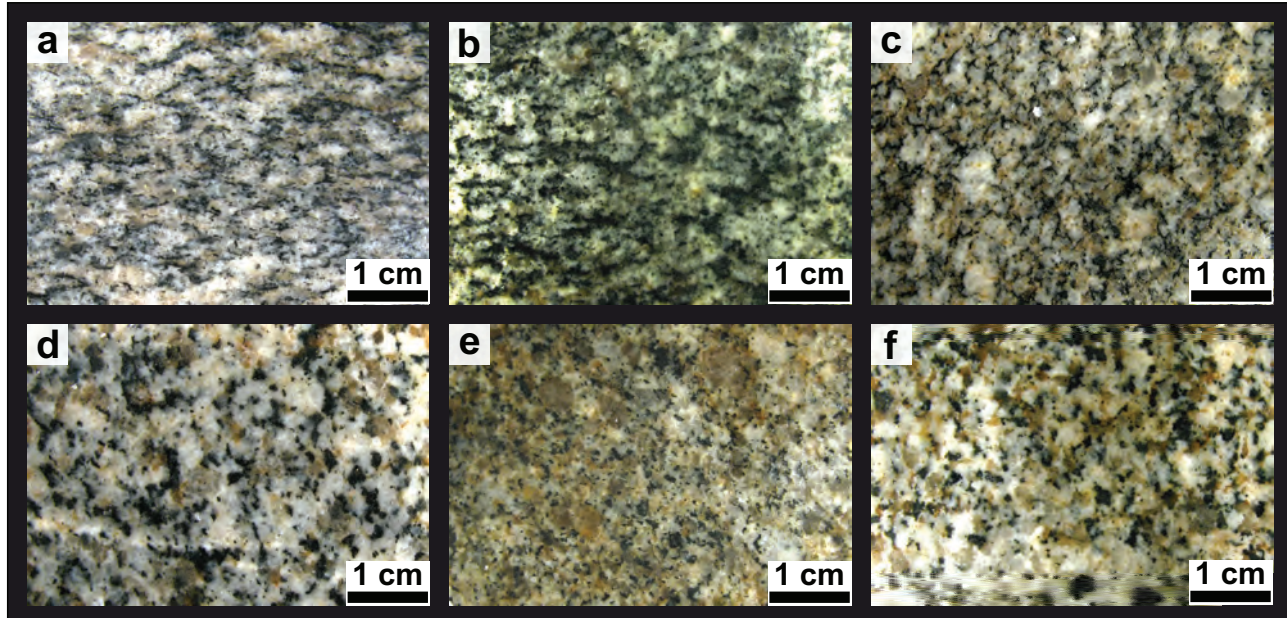


Fig. 2 Sand down surfaces of a representative selection of samples showing the macroscopic variability of the Spitz Gneiss. **a** – Sample ML 16-6, Eitental. **b** – ML 16-20, Gießhübel. **c** – ML 14-10, Eitental. **d** – ML 16-17, Gießhübel. **e** – ML 14-13, Eitental. **f** – ML 16-16, Gießhübel.

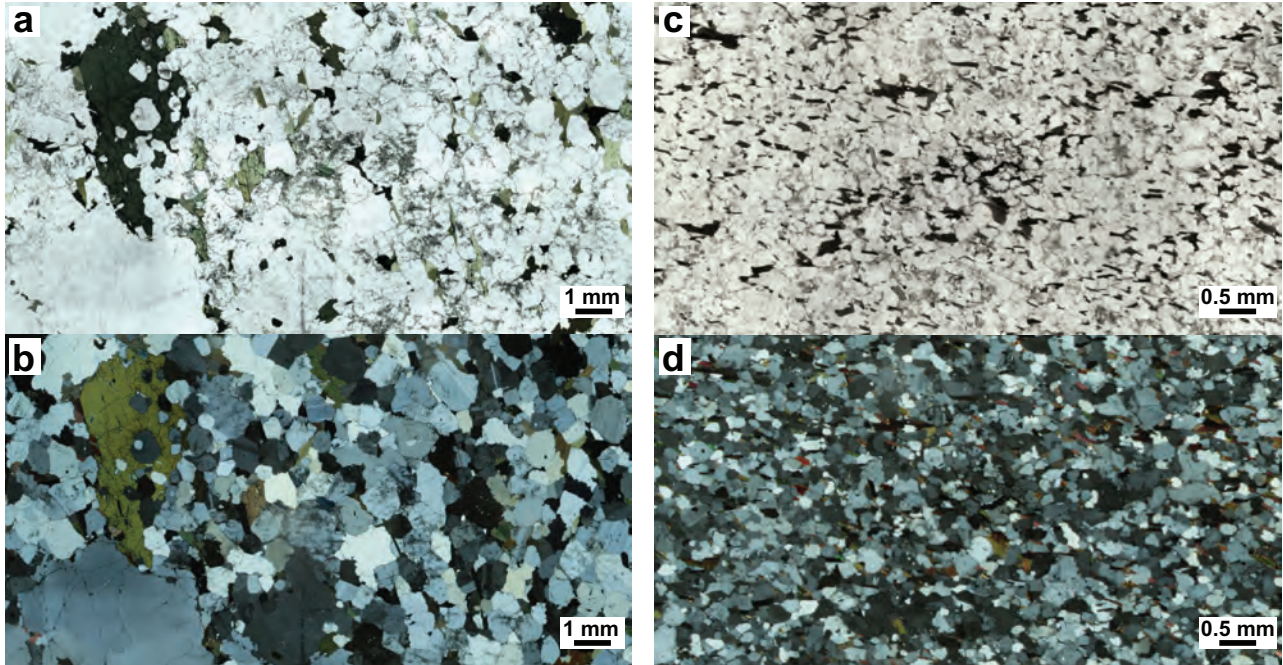


Fig. 3 Thin-section photographs of a medium-grained, amphibole-bearing variety (**a, b**) and a finer grained, biotite-bearing variety (**c, d**) of Spitz Gneiss. Plane- (**a, c**) and cross-polarized light (**b, d**).

4. Petrography of the Spitz Gneiss

Figure 2 gives an overview of the macroscopic variability of the Spitz Gneiss. The rock has a fine to medium grain size. The fabric and the minerals are metamorphic with the exception of some diffuse textural relicts of magmatic feldspar phenocrysts. The foliation is weak to moderate and mainly defined by oriented biotite, more rarely by elongated feldspar or quartz (Fig. 3). The quartz–feldspar fabric is typically granular. Some variants of Spitz Gneiss carry amphibole (Fig. 3a).

Biotite is partly chloritized with fine exsolution lamellae of ilmenite having formed in the chlorite domains. Amphibole, plagioclase and K-feldspar appear homogenous under the optical microscope and in backscattered-electron (BSE) imagery. Small retrograde epidote and muscovite rarely occur along grain boundaries. Accessory minerals are zircon, apatite and allanite.

5. Mineral chemistry and geothermobarometry

5.1. Mineral compositions

Representative analyses are given in Tab. 2. The anorthite content of plagioclase ranges between An₂₃ and An₃₁ in the amphibole-bearing thin section and from An₁₉ to An₂₅

in the more felsic sample. Single plagioclase crystals are compositionally widely homogenous. *K-feldspar* is Na-poor (Ab_{5–10}) and shows BaO contents of ~0.6 to 0.8 wt. %; CaO remained below the detection limit (0.1 wt. %).

Amphibole compositions are uniformly calcic with CaO contents around 11 wt. % and moderate alkali-element concentrations (Na₂O 1.1–1.6 wt. %; K₂O 1.3–1.9 wt. %). Having Mg/(Mg+Fe²⁺) below 0.5 and Si (*apfu*) around 6.5, the amphiboles can be classified as ferroedenite to ferropargasite (Fig. 4b, 5a).

Biotite (Fig. 4a–d, 5b) from the more felsic sample shows Mg/(Mg + Fe) ratios of ~0.5, those in the amphibole-bearing sample ~0.45. The Al^{IV} content (*apfu*) is relatively low (2.0–2.6) in both cases.

The secondary *chlorite* (Fig. 4d) classifies as chamosite (Fig. 5c), with Mg/(Mg + Fe) of 0.49 in the amphibole-free sample and 0.43 in the amphibole-bearing sample. Si (*apfu*) is around 5.65 in the amphibole-free sample and between 5.9 and 6.8 in the amphibole-bearing one. Table 2 includes also an analysis of a rare secondary epidote (Fig. 4b) and a secondary muscovite.

5.2. Mineral thermobarometry

The mineral paragenesis amphibole plus plagioclase (+ Kfs, Qz) is suitable for various geothermobarometric calculations. Using the hornblende–plagioclase geothermometer introduced by Holland and Blundy (1994), in connection with the Al-in-amphibole geobarometer of

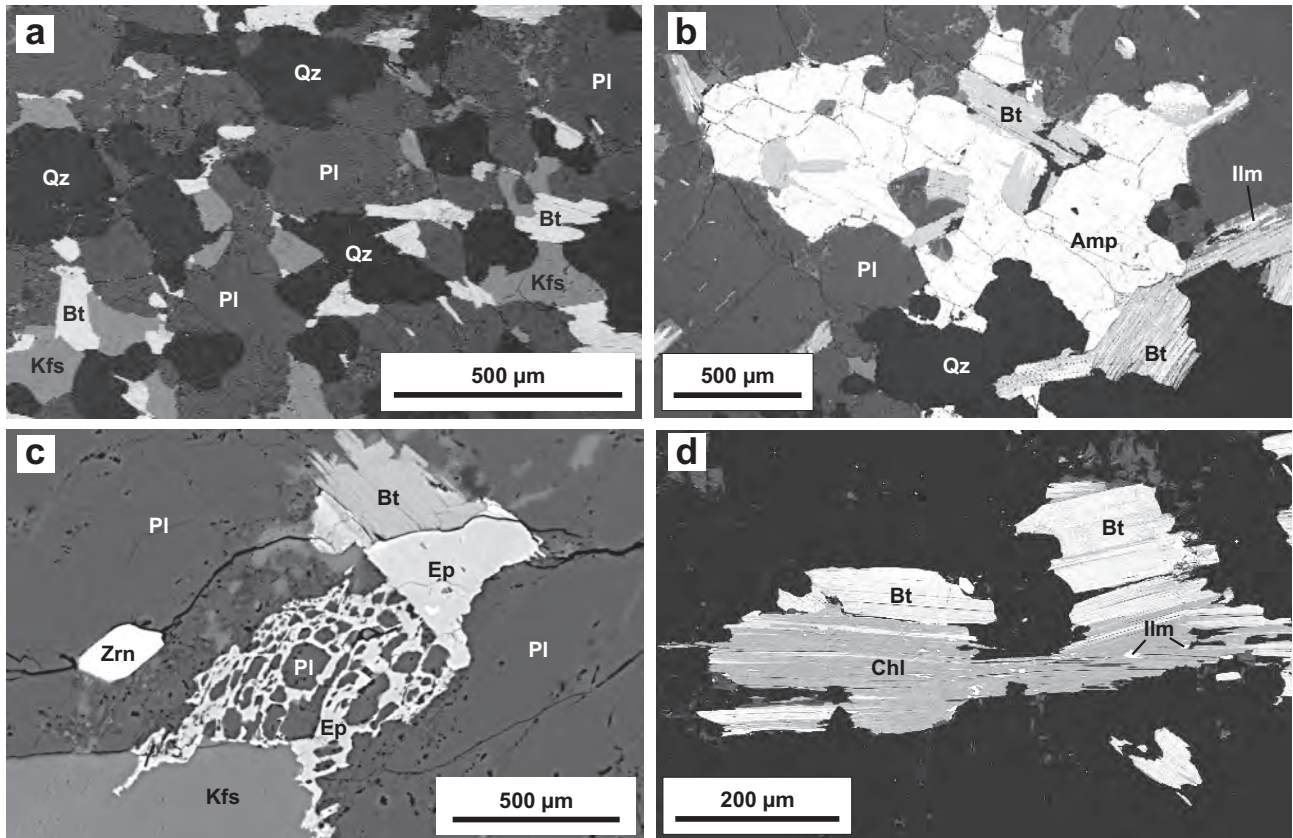


Fig. 4 Scanning electron microscope images (BSE, from thin sections ML 14-1B and ML 14-10. **a** – Typical metamorphic fabric of the Spitz Gneiss with plagioclase, quartz, biotite and K-feldspar (ML 14-1B). **b** – Large amphibole grain with biotite inclusions intergrown with plagioclase; ilmenite exsolution lamellae in chloritized biotite. **c** – Rare example of secondary epidote. **d** – Chloritized biotite with ilmenite exsolution in chlorite. Mineral abbreviations according to Whitney and Evans (2010).

Anderson and Smith (1995), an average temperature of $698 \pm 10^\circ\text{C}$ (2σ) at an average pressure of 6.51 ± 0.25 kbar can be deduced. The application of the empirical Ti-in-

amphibole thermometer of Otten (1984) yields almost the same temperature estimate of 697°C . The Ti-in-biotite thermometer of Henry et al. (2005) gives an average

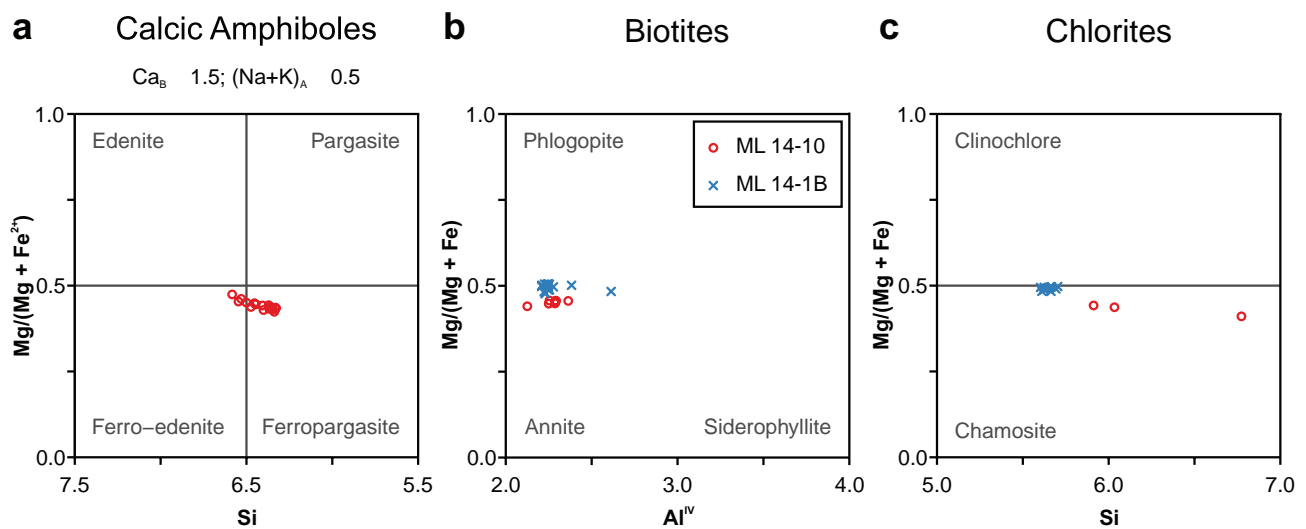


Fig. 5 Mineral chemistry classification diagrams (apfu). **a** – Amphibole classification diagram for calcic amphiboles ($\text{Ca}_B \geq 1.5$; $(\text{Na} + \text{K})_A \geq 0.5$) after Leake et al. (1997). Fe^{2+} calculated from FeO_{tot} after Holland and Blundy (1994). **b** – Biotite classification diagram (Rieder et al. 1999). Total iron calculated as Fe^{2+} . **c** – Chlorite classification diagram (Bayliss 1975). Total iron calculated as Fe^{2+} .

Tab. 2 Representative mineral analyses for Spitz Gneiss samples ML 14-1B and ML 14-10

Sample	ML 14-10				ML 14-10				ML 14-1B				ML 14-1B				Sample	ML 14-10		ML 14-1B		
	Mineral	Amp	Amp	Amp	Bt	Bt	Bt	Ms	Cln	Cln	Chl	Ep	Mineral	Pl	Pl	Pl	Kfs	Kfs				
SiO ₂	42.17	42.74	41.76		38.37	36.84	38.01	47.96	27.88	27.01		37.44	SiO ₂	60.71	61.48	64.85	61.47	65.19	65.02			
TiO ₂	1.02	1.09	1.13		3.36	2.97	2.85	0.59	0.28	0.13		0.64	TiO ₂	n.a.	n.a.	n.a.	n.a.	n.a.	n.a.			
Al ₂ O ₃	12.55	11.36	12.27		14.77	14.38	15.57	30.00	21.86	20.90		22.45	Al ₂ O ₃	24.27	23.60	22.84	22.98	17.94	18.08			
FeO _{tot}	20.15	20.54	20.38		21.78	18.67	19.32	4.60	24.88	25.89		12.90	FeO _{tot}	n.a.	n.a.	n.a.	n.a.	n.a.	n.a.			
MgO	7.34	7.46	7.26		9.94	10.32	10.70	3.23	13.82	13.58		0.22	MgO	n.a.	n.a.	n.a.	n.a.	n.a.	n.a.			
MnO	0.66	0.68	0.70		0.46	0.34	0.27	b.d.l.	0.30	0.47		0.31	MnO	n.a.	n.a.	n.a.	n.a.	n.a.	n.a.			
Na ₂ O	1.55	1.31	1.61		0.23	0.39	0.33	0.19	b.d.l.	b.d.l.		b.d.l.	Na ₂ O	7.95	8.22	9.13	8.78	0.91	0.61			
K ₂ O	1.70	1.57	1.87		9.75	8.89	8.57	10.56	0.41	0.09		0.11	K ₂ O	0.39	0.67	0.37	0.31	14.76	15.01			
CaO	10.84	11.16	10.97		b.d.l.	b.d.l.	b.d.l.	b.d.l.	b.d.l.	b.d.l.		22.67	CaO	6.59	5.22	4.16	4.98	0.00	0.00			
BaO	b.d.l.	b.d.l.	b.d.l.		b.d.l.	b.d.l.	b.d.l.	b.d.l.	b.d.l.	b.d.l.		b.d.l.	BaO	0.13	b.d.l.	b.d.l.	b.d.l.	0.73	0.71			
Total	98.00	97.91	97.96		98.64	92.80	95.76	97.13	89.44	88.08		96.74	Sum	100.04	99.20	101.36	98.52	99.53	99.44			
Number of ions on the basis of:																						
23 O	23 O	23 O			22 O	22 O	22 O	22 O	28 O	28 O		12.5 O	Si	3.02	Si	2.71	2.75	2.83	2.77	3.02	3.02	
Si	6.38	6.48	6.35		Si	5.71	5.75	5.72	6.38	2.85	2.83		3.02	Al	1.28	1.25	1.17	1.17	1.22	0.98	0.99	
Al ^{IV}	1.62	1.52	1.65		Al ^{IV}	2.29	2.25	2.28	1.62	1.15	1.17		Sum	3.98	4.00	4.00	3.99	4.00	4.00	4.00		
Sum	8.00	8.00	8.00		Sum	8.00	8.00	8.00	8.00	4.00	4.00		Sum	8 O	8 O	8 O	8 O	8 O	8 O	8 O		
Al ^{VI}	0.62	0.51	0.55		Al ^{VI}	0.30	0.40	0.49	3.08	1.49	1.41		Al	2.13	Ca	0.32	0.25	0.19	0.24	0.00	0.00	
Ti	0.11	0.12	0.13		Ti	0.38	0.35	0.35	0.32	0.06		Fe ³⁺	0.78	Na	0.69	0.71	0.77	0.77	0.08	0.05		
Fe ^{3+*}	0.43	0.41	0.39									Sum	2.91	K	0.02	0.04	0.02	0.02	0.87	0.89		
Mg	1.66	1.69	1.65		Mg	2.21	2.40	2.40	0.64	2.11	2.12		Ca	1.93	Ba	0.00	0.00	0.00	0.01	0.01		
Mn	0.08	0.09	0.09		Mn	0.06	0.04	0.03	0.00	0.03	0.04		Ti	0.04	Sum	1.03	1.00	0.99	1.02	0.97	0.96	
Fe ^{2+*}	2.10	2.18	2.19		Fe	2.71	2.44	2.43	0.51	2.13	2.27		K	0.01	mol. %							
M1.2,3	5.00	5.00	5.00		Sum	5.66	5.63	5.68	4.29	4.29	4.29		Mg	0.03	An	30.74	24.99	19.68	23.44	0.00	0.00	
Ca	1.76	1.81	1.79		Ca	0.00	0.00	0.02	0.00	0.00	0.00		Mn	0.02	Ab	67.10	71.18	78.23	74.84	8.60	5.81	
Na	0.22	0.17	0.20		Na	0.07	0.12	0.10	0.05	0.05	0.05		Sum	2.03	Or	2.16	3.83	2.09	1.72	91.40	94.19	
Fe	0.02	0.02	0.01		K	1.85	1.77	1.65	1.79	0.05	0.01											
M4	2.00	2.00	2.00		Sum	1.92	1.89	1.77	1.84	1.09	1.05											
Na	0.23	0.21	0.28																			
K	0.33	0.31	0.36																			
A	0.56	0.52	0.64																			
1-A	0.44	0.48	0.36																			

^{*} Fe²⁺ and Fe³⁺ calculated from FeO_{tot} after Holland and Blundy (1994)

Mineral abbreviations according to Whitney and Evans (2010)

temperature of 676 and 678 °C for the two investigated samples. Al-in-amphibole barometry results in 7.11 ± 0.52 kbar (Schmidt 1992) or 6.78 ± 0.47 kbar (Anderson 1996).

Measured chlorite compositions point to a low chlorite formation temperature, for instance 225–240 °C using the chlorite thermometer of Xie et al. (1997) that is based on the temperature dependency of Al^{IV} (Cathelineau 1988) and the linear relationship between Al^{IV} and Fe/(Fe + Mg). Average temperatures of 211 °C at 1 kbar, 221 °C at 2 kbar, or 236 °C at 3 kbar resulted from the model of Lanari et al. (2014) that is based on the Fe–Mg,

Tschermark and di-trioctahedral substitution, assuming all measured Fe is Fe²⁺.

6. Geochemistry of the Spitz Gneiss

6.1. Major-element data

The Spitz Gneiss covers a SiO₂ range from ~64 to ~71 wt. % (Fig. 6, Tab. 3) and it thus represents an intermediate to moderately acidic rock. Amphibole-bearing samples

have commonly less than 68 wt. % SiO₂, amphibole-free samples more than 68 wt. % SiO₂. Many major elements (e.g. FeO, MgO, TiO₂, CaO, Al₂O₃, P₂O₅) show a negative covariation with SiO₂; exceptions are K₂O (rising with increasing SiO₂) and Na₂O (no clear trend). The K₂O/Na₂O ratios are typically 0.3–0.8. Based on the moderate K₂O content (Fig. 6a), the Spitz Gneiss can be classified as “medium-K” (Peccerillo and Taylor 1976); only a few samples are “high-K”.

Applying the classification schemes of Frost et al. (2001), the Spitz Gneiss is magnesian, and subaluminous, i.e. with an aluminium saturation index (ASI) around 1 (Fig. 6b–c). Amphibole-bearing samples are in general slightly metaluminous, amphibole-free samples

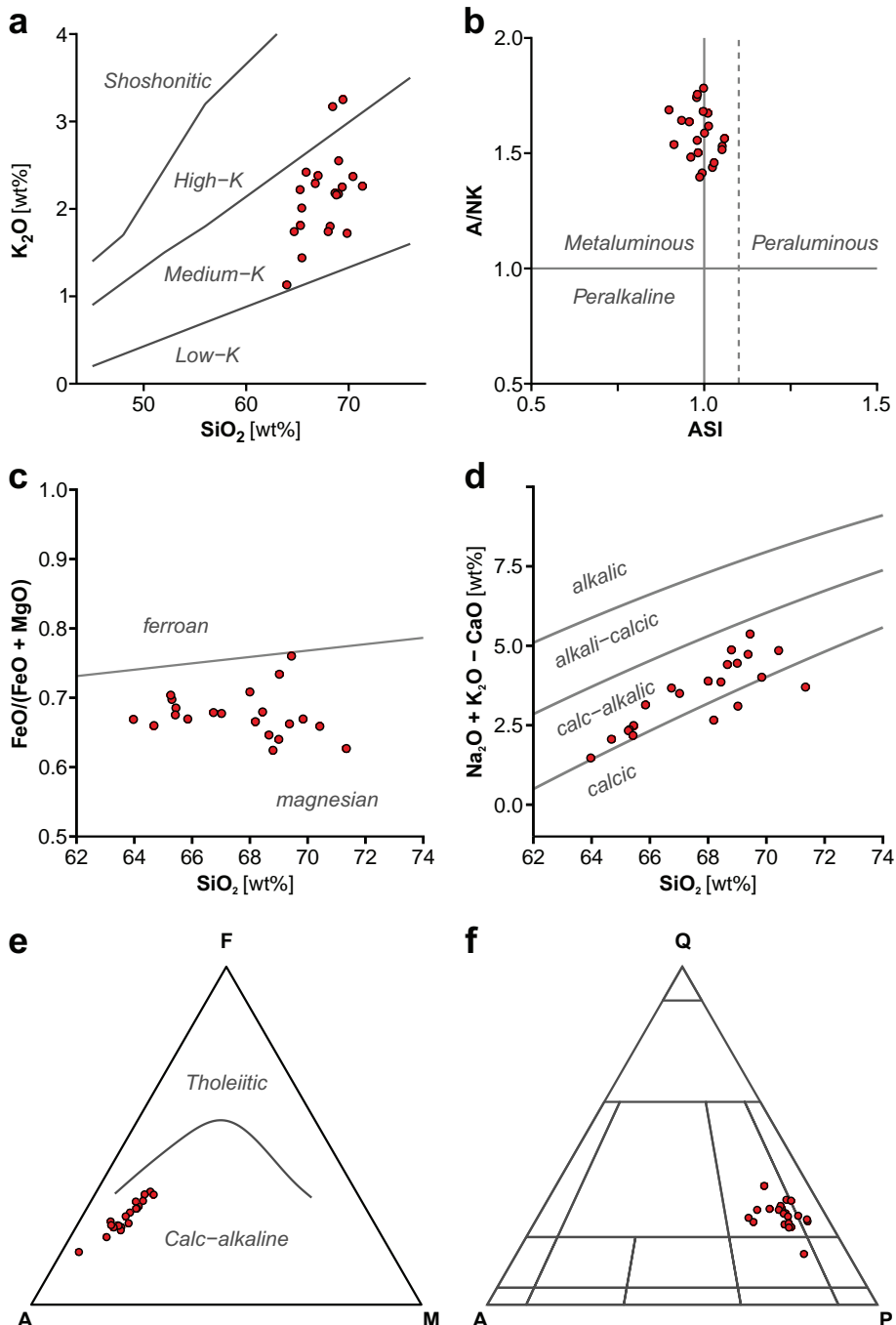


Fig. 6 Various major-element-based classification diagrams for igneous rocks with data from the Spitz Gneiss. **a** – SiO₂ vs. K₂O plot of Peccerillo and Taylor (1976). **b** – ASI vs. A/NK plot of Frost et al. (2001) showing the metaluminous to slightly peraluminous nature. **c** – SiO₂ vs. FeO/(FeO_t + MgO) plot of Frost et al. (2001) illustrating the magnesian character. **d** – SiO₂ vs. Na₂O + K₂O - CaO diagram with fields for alkali, alkali-calcic, calc-alkalic and calcic associations after Frost et al. (2001). **e** – AFM diagram (A = Na₂O + K₂O, F = FeO_t, M = MgO) after Irvine and Baragar (1971) displaying the calc-alkaline trend. **f** – QAP-plot after Streckeisen (1974) from the calculated mesonormative compositions (Mielke and Winkler 1979). Most samples fall within the granodiorite field.

Tab. 3 Representative whole-rock major- (wt. %) and trace-element (ppm) compositions for Spitz Gneiss samples

Sample	a	b	c	d	e	f	g	h
	Amphibole-bearing				Amphibole-free			
	ML 16-28	ML 16-33	ML 14-8	ML 16-6	ML 14-10	ML 16-27	ML 14-1A	ML 16-16
Coordinates	N E	48.379555 15.350658	48.401523 15.389478	48.359276 15.365541	48.258377 15.275041	48.262578 15.275880	48.358024 15.384578	48.359179 15.365783
SiO ₂	63.97	64.68	65.30	66.74	67.02	68.00	68.66	68.44
Al ₂ O ₃	17.78	16.99	16.51	16.73	16.62	16.55	16.40	16.23
MnO	0.05	0.06	0.07	0.07	0.07	0.05	0.04	0.04
MgO	1.46	1.87	1.57	1.30	1.35	0.95	1.25	1.05
CaO	5.32	4.42	4.37	3.65	3.56	3.49	2.85	3.44
Na ₂ O	5.66	4.74	4.92	5.03	4.68	5.64	5.08	4.13
K ₂ O	1.13	1.74	1.81	2.29	2.38	1.74	2.18	3.17
TiO ₂	0.54	0.56	0.54	0.42	0.41	0.33	0.34	0.36
P ₂ O ₅	0.17	0.16	0.14	0.13	0.14	0.12	0.13	0.11
Fe ₂ O ₃	3.64	4.48	4.47	3.39	3.50	2.85	2.82	2.75
SO ₃	0.02	0.01	0.03	0.02	0.02	0.01	0.01	0.01
F	0.12	0.14	0.13	0.11	0.12	0.11	0.11	0.09
LOI	0.87	0.62	0.64	0.52	1.01	0.73	1.12	1.00
Sum	100.73	100.47	100.50	100.40	100.88	100.57	100.99	100.82
X-ray fluorescence analysis (University of Salzburg, Austria)								
Rb	22	66	62	73	79	46	87	97
Sr	492	417	358	269	248	422	331	358
Ba	396	354	455	418	422	541	426	912
Ga	22	20	18	19	19	19	20	17
Nb	9	10	9	7	7	8	7	7
Zr	172	166	136	125	138	133	119	131
Y	11	12	16	13	19	11	11	7
Sc	11	8	11	7	8	7	bdl	bdl
Pb	8	8	7	6	11	10	7	bdl
Zn	34	67	58	61	67	69	29	46
V	43	45	68	47	43	28	49	22
Co	4	8	7	3	3	4	4	4
Cr	23	37	18	22	16	17	30	20
Ni	9	13	8	6	5	6	9	9
La		10.3	19.1		22.1		10.6	
Ce		44.4	45.6		45.9		25.1	
Pr		2.79	4.85		5.33		2.56	
Nd		10.0	17.1		18.7		8.2	
Sm		2.43	3.57		3.54		1.57	
Eu		1.03	0.99		1.03		0.74	
Gd		2.57	3.09		3.38		1.54	
Tb		0.42	0.49		0.51		0.28	
Dy		2.41	2.86		3.29		1.69	
Ho		0.47	0.68		0.69		0.38	
Er		1.20	1.66		2.01		1.01	
Tm		0.15	0.23		0.31		0.16	
Yb		1.02	1.61		1.97		1.14	
Lu		0.18	0.24		0.34		0.20	
Hf		4.5	4.2		4.0		3.3	
U		0.93	2.61		1.38		1.81	
Th		7.89	7.03		6.76		5.85	
Cs		1.47	0.95		1.45		1.14	
Ta		0.4	0.6		0.5		0.3	

a-d – amphibole-bearing samples; e-h – amphibole-free samples

bdl = below detection limit, LOI = loss on ignition

slightly peraluminous. A/NK ratios range between 1.36 and 1.63 (Fig. 6b). The $\text{Na}_2\text{O} + \text{K}_2\text{O}$ – CaO values are mainly in the calc-alkalic range *sensu* Frost et al. (2001) (Fig. 6d). In the AFM diagram after Irvine and Baragar (1971), the Spitz Gneiss follows the calc-alkaline differentiation trend (Fig. 6f). All these geochemical parameters are characteristic of I-type granitoids (Chappell and White 1974).

Primary modal compositions, calculated using the Mesonorm model (Mielke and Winkler 1979; implemented in the *GCDkit* by Janoušek et al. 2006), indicate strong

plagioclase dominance. The Spitz Gneiss protolith can thus be described as quartz-poor granodiorite, transitional to tonalite (Fig. 6e). The primary biotite contents are estimated between 6 and 15 % and a small amount of normative amphibole is present (up to 6 %) in the low SiO_2 samples, consistent with microscopic observations.

6.2. Trace-element data

Some trace elements like Zr or Nb show a negative correlation with SiO_2 (Fig. 7a–b). The Zr content falls from ~170 ppm to ~100 ppm, documenting zircon saturation of the magma and early zircon precipitation during magmatic crystallization (Chappell et al. 1998; Miller et al. 2003).

Srtonium, although generally a compatible element in granitoids, lacks a clear negative correlation trend with SiO_2 . A possibly bimodal data distribution in a SiO_2 vs Sr diagram (Fig. 7c) may indicate that the more mafic and the more felsic samples of Spitz Gneiss had different parental magmas or even sources. On the other hand, Sr is potentially mobile during metamorphism and the original magmatic covariations could be disturbed.

Ba shows concentrations consistently around 400 ppm in the less felsic samples, but scatters widely between 300 and 800 ppm in the more felsic samples (Fig. 7d). Rubidium increases with the SiO_2 content, and shows a good correlation with K_2O (Fig. 7e), as is often observed in igneous systems.

In the trace-element discrimination diagram of Pearce et al. (1984), the Spitz Gneiss falls within the field of volcanic-arc

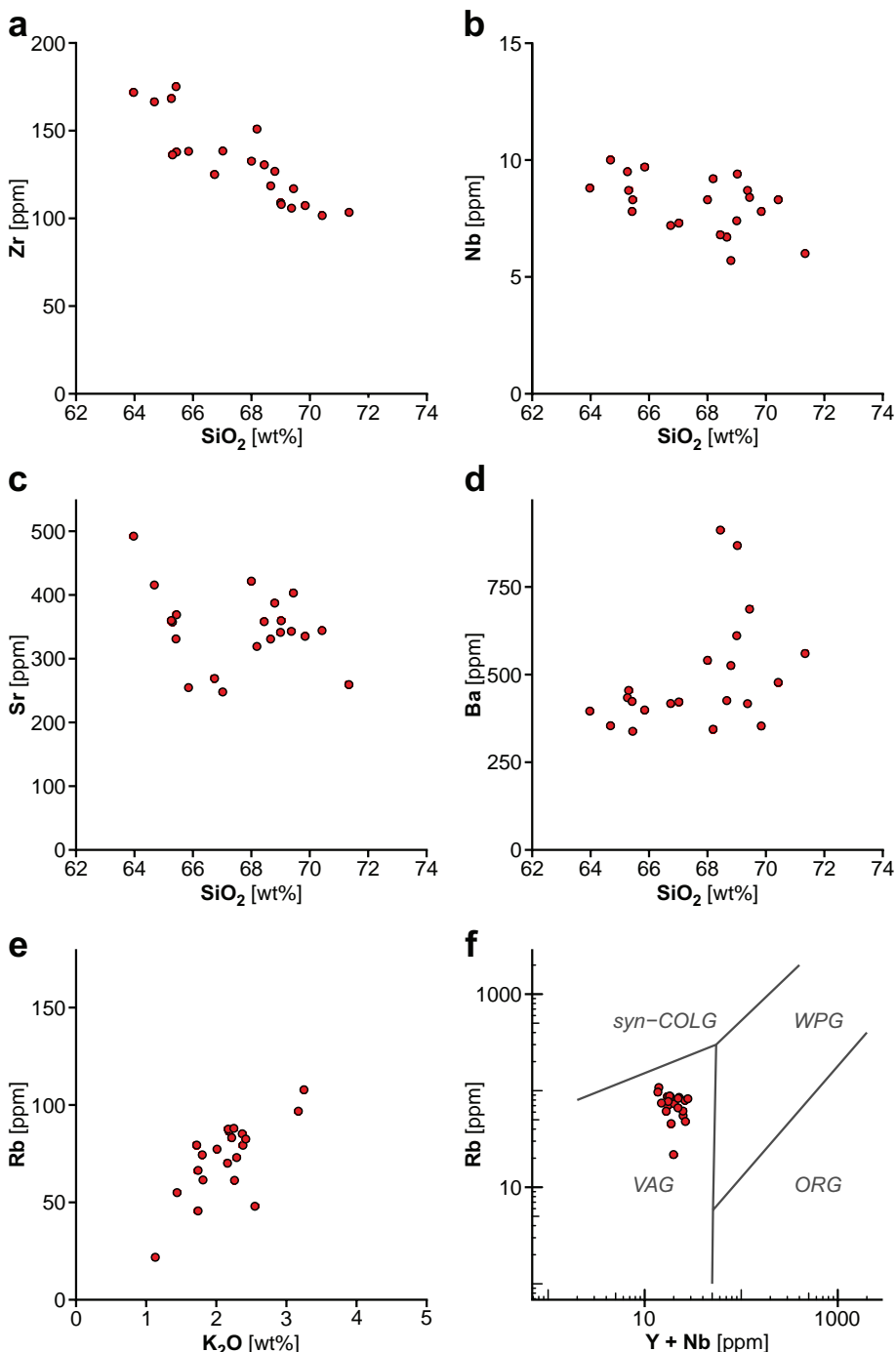


Fig. 7a–d – Binary plots of SiO_2 vs. Zr, Nb, Sr and Ba. **e** – K_2O vs. Rb diagram showing the positive correlation of both elements. **f** – $\text{Y} + \text{Nb}$ vs. Rb diagram after Pearce et al. (1984). Spitz Gneiss samples fall within the volcanic-arc field.

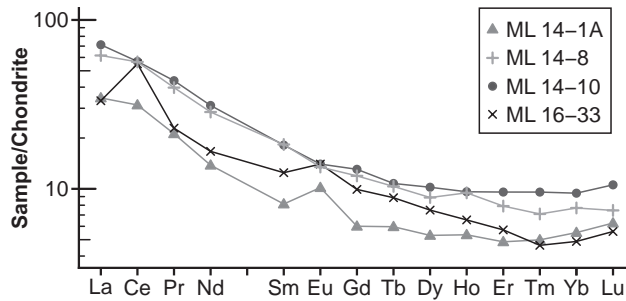


Fig. 8 Chondrite-normalized REE multi-element plot for Spitz Gneiss samples (normalizing values from Boynton 1984).

granites (Fig. 7f), which is in accordance with its I-type characteristics.

Chondrite-normalized Rare Earth Element (REE) patterns (Boynton 1984) for four representative samples of Spitz Gneiss are shown in Fig. 8. All samples have moderate LREE enrichment, decreasing from La (33–70 La_N) to Sm (8–18 Sm_N). The HREE tails of the patterns are flat (5.9–10.7 Tb_N; 5.6–10.6 Lu_N). Samples ML 14-1A and ML 16-33 have a slight positive Eu anomaly and thus likely have experienced magmatic feldspar accumulation. The rare feature of a positive Ce anomaly is observed in sample ML 16-33. It may result from the addition of Ce⁴⁺ from a fluid (Starýš Mayer et al. 2014). Finds of cerianite (CeO₂) in a pegmatite in the vicinity of sample ML 16-33 (Walter et al. 2017) are an indication for a local fractionation and mobility of Ce⁴⁺. The problem regarding the Ce anomaly appears interesting and would deserve a more detailed future study including LA-ICP-MS measurements on single rock-forming minerals.

Figure 9 shows an N-MORB normalized multi-element plot for the Spitz Gneiss. There is a moderately strong enrichment of the Large Ion Lithophile Elements (LILE; e.g. Cs, Rb, Ba, K) at an only slight to moderate enrichment of the HFSE and the LREE. We observe troughs for Nb, Ta, P and Ti, as well as spikes for K, Pb and Sr. The HREE (Gd–Lu) and Y are slightly depleted relative to N-MORB. The enrichment of LILE over Nb and Ta, in combination with a relative depletion in HFSE, is characteristic of most granodioritic rocks world-wide and the Spitz Gneiss is no exception in this respect. We can state though, that the enrichment of Cs in the Spitz Gneiss is less pronounced than in many other granodiorites (e.g. Variscan granodiorites from the Bohemian Massif – Janoušek et al. 2000; Laurent et al. 2014). Conversely, the LREE/HREE enrichment is rather modest in the Spitz Gneiss, while the depletion in the HREE is pronounced relative to the average granodiorite (Taylor 1968).

7. Discussion and conclusions

7.1. Geochemical comparison of the Spitz Gneiss and the Moravo–Silesian granitoids

The Late Proterozoic Moravo–Silesian granitoids are well investigated with some 200 geochemical data being available in the literature (van Breemen et al. 1982; Finger et al. 1989, 1995, 2000; Souček et al. 1992; Jelínek and Dudek 1993; Hanžl and Melichar 1997; Leichmann

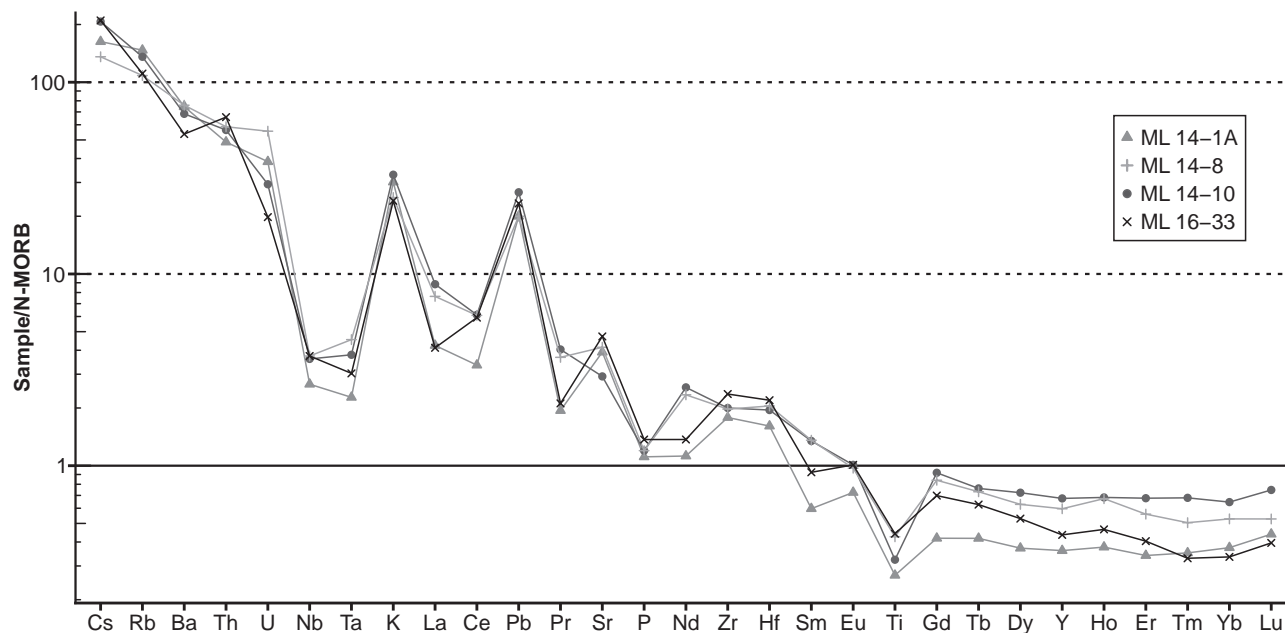


Fig. 9 Multi-element plot normalized by N-MORB (normalizing values from Sun and McDonough 1989).

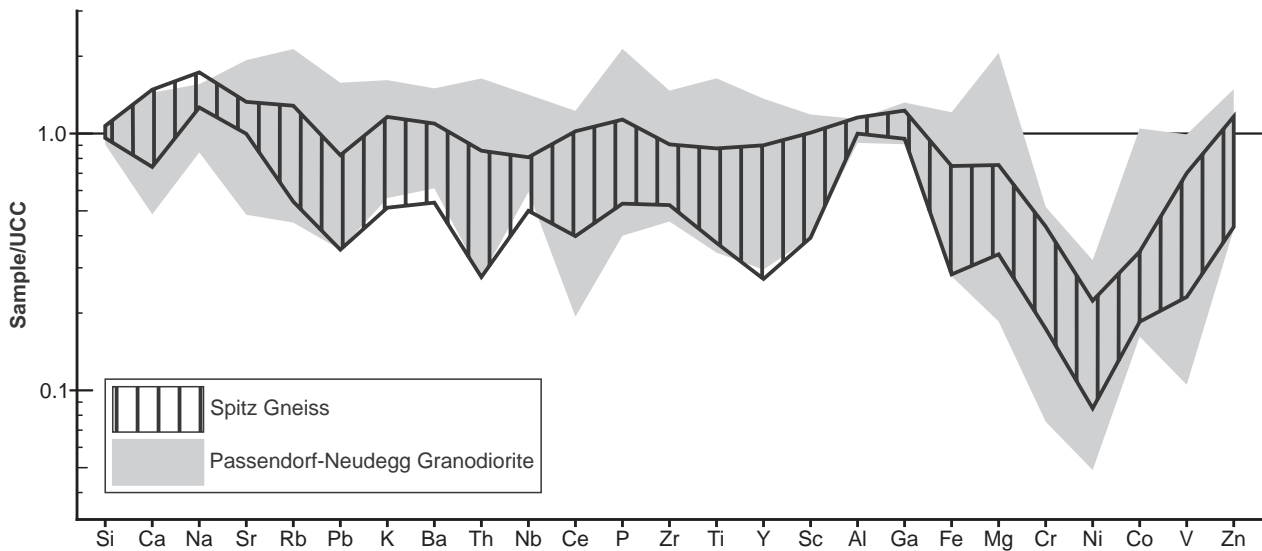


Fig. 10 Multi-element plot illustrating the similarities of Spitz Gneiss (hatched field; $n = 21$) and Passendorf-Neudegg Granodiorite (grey field; $n = 42$). Normalization to average upper continental crust (UCC; Rudnick and Gao 2003).

and Höck 2008; Finger and Riegler 2012a, b; Matzinger and Finger 2017; Soejono et al. 2017). Discrete bodies of I-type biotite \pm hornblende granodiorite were described from several places (Štelcl and Weiss 1986; Finger et al. 1989; Leichmann and Höck 2008; Soejono et al. 2017). Some of these Moravo–Silesian granitoid occurrences are geochemically distinct from the Spitz granodiorite gneiss, as for instance the high-K, Ba- and Cr-rich Buttendorf granodiorite gneiss (Finger and Riegler 2012b, c), the Sr-rich Blansko granodiorite (Hanžl and Melichar 1997;

Leichmann and Höck 2008), the Ba-rich granodiorite from Anenský mlýn (Soejono et al. 2017), or the Zr-rich, high-K Gumping granodiorite (Finger and Riegler 2009, 2012c). However, a good geochemical match is found between the Spitz Gneiss and the Passendorf-Neudegg granodiorite suite in the Thaya Batholith (Finger and Riegler 2006, 2012a), as is shown in Fig. 10.

7.2. Geochemical comparison of Spitz Gneiss and Dobra Gneiss

The term Spitz Gneiss was first used by Waldmann (1938), but a “hornblende-bearing granodioritic gneiss in the surroundings of Spitz” has already been mentioned in earlier work (Becke 1917). The Spitz Gneiss and the Dobra Gneiss were long considered to be the same rock type (e.g. Waldmann 1951; Desphande and Özpeker 1965). However, Fuchs and Matura (1976) defined the Spitz Gneiss as a separate unit due to the fact that it has a significantly lower K-feldspar content than the Dobra Gneiss.

Notably, intercalations of amphibolite (0.5–10 m) are sometimes observed in the Spitz Gneiss (Lindner 2016). They have been interpreted as pre-Variscan mafic dykes (Finger and Steyrer 1995), but their precise age is unknown.

As has been shown in a recent MSc thesis (Lindner 2016), the Dobra Gneiss is also an I-type granitoid, but differs from the Spitz Gneiss in a number of geochemical parameters. Most significant is its higher SiO_2 content (Fig. 11) and its more ferroan nature (Frost et al. 2001). A striking geochemical affinity exists between parts of the Dobra Gneiss and the Moravian Bittesch Gneiss (Lindner and Finger 2016).

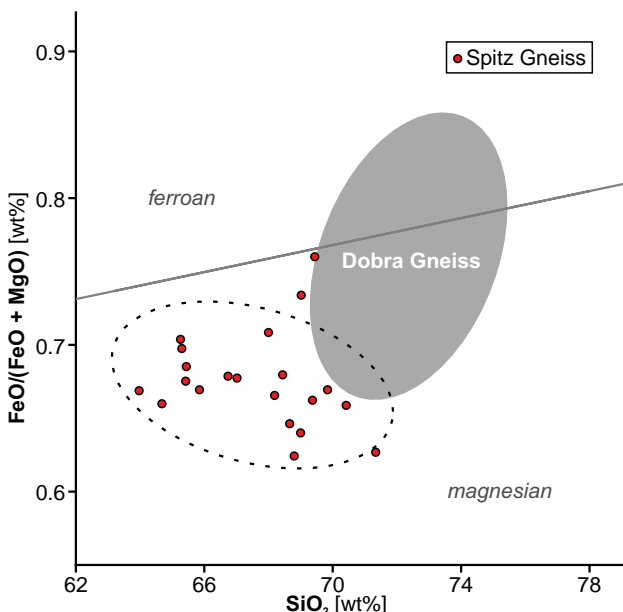


Fig. 11 The SiO_2 - $\text{FeO}/(\text{FeO} + \text{MgO})$ diagram after Frost et al. (2001) showing the distinct chemical characters of the Dobra Gneiss (grey field) and the Spitz Gneiss (dashed field). The two ellipses outline 90 % of the Spitz and Dobra Gneiss data, respectively.

7.3. Comparing the Cadomian to Early Paleozoic magmatism in the Moravo-Silesian and the Moldanubian domains

Based on available literature and unpublished University of Salzburg data, we made an attempt to discriminate the Cadomian Moravo-Silesian granitoid province from the Cadomian to Early Palaeozoic granitoids that are preserved as orthogneiss in the Moldanubian Zone (i.e. Gföhl Gneiss, Blaník Gneiss, Stráž Gneiss, Vír/Svratka Gneiss, Orlice-Sněžník Gneiss; van Breemen et al. 1982; Souček et al. 1992; Vellmer 1992; Breiter et al. 2005; Hasalová et al. 2008; Buriánek et al. 2009; René and Finger 2016). The Moldanubian orthogneisses have, on average, higher A/CNK values, higher Y and HREE and lower Ba values. The best discrimination is provided in the Rb vs. Sr diagram (Fig. 12). Most Moravo-Silesian granitoids have Sr > 200 ppm and Rb < 200 ppm, while the Moldanubian orthogneisses have invariably Sr < 200 ppm and Rb often exceeds 200 ppm. Both, the Spitz and the Dobra Gneiss, fall clearly within the field of the Moravo-Silesian granitoids.

7.4. Tectonic implications

The fact that the Spitz Gneiss fits reasonably well into the compositional and age spectrum of the Cadomian granitoids of the Moravo-Silesian Unit corroborates geological models claiming that the Lower Austrian Drosendorf Unit belonged to the Moravian Zone (and to Avalonia) before it was tectonically incorporated into the Moldanubian nappe system (Fritz and Neubauer 1993; Finger et al. 2007b). Notably, temporal and compositional equivalents to the Spitz Gneiss (as well as to the Dobra Gneiss) have not yet been found elsewhere in the Moldanubian Zone, whereas the most characteristic Moldanubian S-type orthogneisses (Gföhl Gneiss and Blaník Gneiss) are totally absent in the Drosendorf Unit. All this highlights the exotic nature of the Lower Austrian Drosendorf Unit.

During the Variscan Orogeny, the Drosendorf Unit inevitably experienced significantly higher regional metamorphic conditions than the Moravian Unit in the Austrian part of the Thaya Dome. Our peak P-T estimates for the Spitz Gneiss (~700 °C, 7 kbar) are in accord with previous geothermobarometric data from other parts of the Lower Austrian Drosendorf Unit (Högelsberger 1989), whereas maximum P-T conditions of around 600 °C, 6 kbar have been reported from the hanging-wall parts of the Moravian Unit in Austria (Höck et al. 1990). Based on the Variscan metamorphic conditions it would make sense to interpret the Drosendorf Unit as a westerly and thus hotter part of the subducted Moravian Plate that was ripped off and steeply exhumed into the overlying

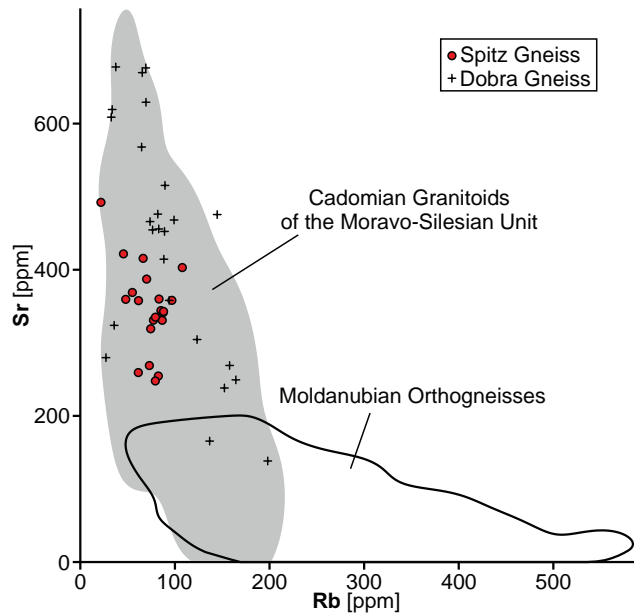


Fig. 12 Rb vs. Sr scatterplot for Moldanubian orthogneisses and the Cadomian granitoids of the Moravo-Silesian Unit. Dobra and Spitz Gneiss are independently plotted and fall within the Moravo-Silesian field. Fields represent 90 % of the input data, based on a 2D kernel density estimation (Venables and Ripley 2002). (Data sources: van Breemen et al. 1982; Souček et al. 1992; Vellmer 1992; Jelínek and Dudek 1993; Hanzl and Melichar 1997; Finger et al. 2000; Breiter et al. 2005; Leichmann and Höck 2008; Hasalová et al. 2008; Buriánek et al. 2009; Finger and Riegler 2012a, b, c, 2013, 2014; René and Finger 2016; Matzinger and Finger 2017; Soejono et al. 2017 and additional unpublished data of the University of Salzburg).

Moldanubian Plate during the Variscan Orogeny, possibly through processes of backthrusting (Fritz and Neubauer 1993). In terms of metamorphic conditions, the Drosendorf Unit may correspond to the Vranov-Olešnice Unit in the Czech part of the Moravian Unit.

The Variscan exhumation of the Spitz Gneiss (and probably of the entire Lower Austrian Drosendorf Unit) to upper crustal levels was likely a fast process, because minerals like hornblende and plagioclase lack retrograde reequilibration at lower amphibolite- and upper greenschist-facies conditions. A fast cooling of the unit at ~340 Ma has also been inferred by Dallmeyer et al. (1992) and Racek et al. (2017) based on Ar-Ar mica and hornblende dating. The observable chloritization of biotite in the Spitz Gneiss represents a post-exhumation event at ~250 °C. It was probably triggered by a regional fluid introduction into the post-collisional Variscan crust (Jawecki 1996), during the Carboniferous or Permian.

Acknowledgements. This work is based on the master's thesis of M.L. at the University of Salzburg. Helpful comments by reviewers K. Breiter, E. Jelínek and V. Kachlík are gratefully acknowledged, as well as stylistic and linguistic improvements of the manuscript by C. Geiger. We thank M. Svojtka and V. Janoušek for careful edito-

rial handling of the manuscript. M.L. is a recipient of a DOC Fellowship of the Austrian Academy of Sciences.

Electronic supplementary material. Supplementary table of whole-rock chemical compositions from the Spitz Gneiss is available online at the Journal web site (<http://dx.doi.org/10.3190/jgeosci.271>).

References

- ANDERSON JL (1996) Status of thermobarometry in granitic batholiths. *Trans Roy Soc Edinb, Earth Sci* 87: 125–138
- ANDERSON JL, SMITH DR (1995) The effects of temperature and fO_2 on the Al-in-hornblende barometer. *Amer Miner* 80: 549–559
- BAYLISS P (1975) Nomenclature of the trioctahedral chlorites. *Canad Mineral* 13: 178–180
- BECKE F (1917) Granodioritgneis im Waldviertel. *Tschermaks mineral petrogr Mitt* 34: 70
- BOYNTON W V (1984) Cosmochemistry of the rare earth elements: meteorite studies. In: HENDERSON P (ed) *Rare Earth Element Geochemistry*. Elsevier, Amsterdam, pp 63–114
- BREITER K (2010) Geochemical classification of Variscan granitoids in the Moldanubicum (Czech Republic, Austria). *Abh Geol B -A* 65: 19–25
- BREITER K, SCHARBERT S (2006) Two-mica and biotite granites in the Weitra–Nové Hrady area, Austria–Czech Republic. *J Czech Geol Soc* 51: 217–230
- BREITER K, ČOPJAKOVÁ R, GABAŠOVÁ A, ŠKODA R (2005) Chemistry and mineralogy of orthogneisses in the northeastern part of the Moldanubicum. *J Czech Geol Soc* 50: 81–94
- BURIÁNEK D, VERNER K, HANŽL P, KRUMLOVÁ H (2009) Ordovician metagranites and migmatites of the Svatka and Orlice–Snežník units, northeastern Bohemian Massif. *J Geosci* 54: 181–200
- CATHELINEAU M (1988) Cation site occupancy in chlorites and illites as a function of temperature. *Clay Miner* 23: 471–485
- CHAPPELL B, BRYANT CJ, WYBORN D, WHITE AJR, WILLIAMS IS (1998) High- and low-temperature I-type granites. *Resour Geol* 48: 225–235
- CHAPPELL BW, WHITE AJR (1974) Two contrasting granite types. *Pacif Geol* 8: 173–174
- COOKE RA, O'BRIEN PJ, CARSWELL DA (2000) Garnet zoning and the identification of equilibrium mineral compositions in high-pressure–temperature granulites from the Moldanubian Zone, Austria. *J Metamorph Geol* 18: 551–569
- DALLMEYER RD, NEUBAUER F, HöCK V (1992) Chronology of late Paleozoic tectonothermal activity in the south-eastern Bohemian Massif, Austria (Moldanubian and Moravo–Silesian zones): $^{40}\text{Ar}/^{39}\text{Ar}$ mineral age controls. *Tectonophysics* 210: 135–153
- DESPHANDE GG, ÖZPEKER I (1965) Petrology and structure of the Spitzer Gneiss from Dobra area in the Bohemian Massif of Austria. *Verh Geol B-A* A77
- DÖRR W, ZULAUF G, FIALA J, FRANKE W, VEJNAR Z (2002) Neoproterozoic to Early Cambrian history of an active plate margin in the Teplá–Barrandian Unit – a correlation of U–Pb isotopic-dilution-TIMS ages (Bohemia, Czech Republic). *Tectonophysics* 352: 65–85
- DUDEK A (1980) The crystalline basement block of the outer Carpathians in Moravia. *Rozpr Čs Akad Věd* 90: 1–85
- FARYAD SW, RACEK M, LEXA O (2011) Eclogite, garnet peridotite, garnet pyroxenite and HP granulite in the Gföhl Unit. *Geolines* 23: 106–111
- FINGER F (1990) Geochemie und primäres tektonisches Environment der granitoiden Gneise des Waldviertler Moldanubikums. In: NEUBAUER F, HOINKES G, WALLBRECHER E, FRITZ H, UNZOG W (eds) *TSK III 3. Symposium für Tektonik, Struktur- und Kristallingeologie*. Zentralbl Geol Paläont Teil I, Graz, pp 58–60
- FINGER F, RIEGLER G (2006) Bericht 2005 über petrographische und geochemische Untersuchungen an Metagranitoiden und Orthogneisen des Moravikums auf Blatt 21 Horn. *Jb Geol B-A* 146: 123–126
- FINGER F, RIEGLER G (2009) Bericht 2008 über petrographische und geochemische Untersuchungen an Metagranitoiden und Orthogneisen des Moravikums auf Blatt 21 Horn. *Jb Geol B-A* 149: 509–512
- FINGER F, RIEGLER G (2012a) Bericht 2009 über petrographische und geochemische Untersuchungen an Metagranitoiden und Orthogneisen des Moravikums auf Blatt 21 Horn. *Jb Geol B-A* 152: 213–216
- FINGER F, RIEGLER G (2012b) Bericht 2010 über petrographische und geochemische Untersuchungen an Metagranitoiden und Orthogneisen des Moravikums auf Blatt 21 Horn. *Jb Geol B-A* 152: 216–218
- FINGER F, RIEGLER G (2012c) Bericht 2011 über petrographische und geochemische Untersuchungen an Metagranitoiden und Granitgneisen des Moravikums auf Blatt 21 Horn. *Jb Geol B-A* 152: 218–220
- FINGER F, RIEGLER G (2013) Bericht 2012 über petrographische und geochemische Untersuchungen an Graniten und Orthogneisen des Moravikums auf Blatt 21 Horn. *Jb Geol B-A* 153: 361–364
- FINGER F, RIEGLER G (2014) Bericht 2013 über petrographische und geochemische Untersuchungen an Orthogneisen des Moravikums auf Blatt 21 Horn. *Jb Geol B-A* 154: 255–258
- FINGER F, STEYRER HP (1995) A tectonic model for the Eastern Variscides – indications from a chemical study of amphibolites in the south-eastern Bohemian Massif. *Geol Carpath* 46: 137–150

- FINGER F, FRASL G, HÖCK V, STEYRER HP (1989) The granitoids of the Moravian Zone of northeast Austria: products of a Cadomian active continental margin? *Precambr Res* 45: 235–245
- FINGER F, FRASL G, DUDEK A, JELÍNEK E, THÖNI M (1995) Cadomian plutonism in the Moravo–Silesian basement. In: DALLMEYER RD, FRANKE W, WEBER K (eds) *Tectonostratigraphic Evolution of the Central and Eastern European Orogens*. Springer, Berlin, pp 495–507
- FINGER F, ROBERTS M, HAUNSCHMID B, SCHERMAIER A, STEYRER HP (1997) Variscan granitoids of central Europe: their typology, potential sources and tectonothermal relations. *Mineral Petrol* 61: 67–96
- FINGER F, HANŽL P, PIN C, von QUADT A, STEYER HP (2000) The Brunovistulian: Avalonian Precambrian sequence at the eastern end of the Central European Variscides? In: FRANKE W, HAAK V, ONCKEN O, TANNER D (eds) *Orogenic Processes: Quantification and Modelling in the Variscan Belt*. Geological Society of London, Special Publications 179: pp 103–112
- FINGER F, GERDES A, KNOP E (2007a) Constraints on the sedimentation age of the Monotonous Series in the Austrian part of the Bohemian Massif from U–Pb Laser ICP-MS zircon dating. *Mitt Österr Mineral Gesell* 153: 43
- FINGER F, GERDES A, JANOUŠEK V, RENÉ M, RIEGLER G (2007b) Resolving the Variscan evolution of the Moldanubian sector of the Bohemian Massif: the significance of the Bavarian and the Moravo–Moldanubian tectono-metamorphic phases. *J Geosci* 52: 9–28
- FRANKE W (1989) Variscan plate tectonics in Central Europe – current ideas and open questions. *Tectonophysics* 169: 221–228
- FRANKE W (2000) The mid-European segment of the Variscides: tectonostratigraphic units, terrane boundaries and plate tectonic evolution. In: FRANKE W, HAAK V, ONCKEN O, TANNER D (eds) *Orogenic Processes: Quantification and Modelling in the Variscan Belt*. Geological Society, London, Special Publications 179: pp 35–61
- FRANKE W, ŹELAŽNIEWICZ A (2000) The eastern termination of the Variscides: terrane correlation and kinematic evolution. In: FRANKE W, HAAK V, ONCKEN O, TANNER D (eds) *Orogenic Processes: Quantification and Modelling in the Variscan Belt*. Geological Society, London, Special Publications 179: pp 63–86
- FRASL G (1970) Zur Metamorphose und Abgrenzung der Moravischen Zone im niederösterreichischen Waldviertel. *Nachr Dtsch geol Gesell* 2: 55–61
- FRASL G (1991) Das Moravikum der Thaya-Kuppel als Teil der variszisch deformierten Randzone des Bruno-Vistulikums – eine Einführung. In: GATTINGER ET, ROETZEL R (eds) *Geologie am Ostrand der Böhmisches Masse in Niederösterreich, Schwerpunkt Blatt 21 Horn*. Geologische Bundesanstalt, Vienna, pp 49–62
- FRIEDEL G, FINGER F, McNAUGHTON NJ, FLETCHER IR (2000) Deducing the ancestry of terranes: SHRIMP evidence for South America-derived Gondwana fragments in central Europe. *Geology* 28: 1035–1038
- FRIEDEL G, FINGER F, PAQUETTE JL, von QUADT A, McNAUGHTON NJ, FLETCHER IR (2004) Pre-Variscan geological events in the Austrian part of the Bohemian Massif deduced from U–Pb zircon ages. *Int J Earth Sci* 93: 802–823
- FRITZ H (1995) The Raabs Series: a probable Variscan suture in the SE Bohemian Massif. *Jb Geol B-A* 138: 639–653
- FRITZ H, NEUBAUER F (1993) Kinematics of crustal stacking and dispersion in the south-eastern Bohemian Massif. *Geol Rundsch* 82: 556–565
- FROST BR, BARNES CG, COLLINS WJ, ARCUS RJ, ELLIS DJ, FROST CD (2001) A geochemical classification for granitic rocks. *J Petrol* 42: 2033–2048
- FUCHS G (1976) Zur Entwicklung der Böhmischen Masse. *Jb Geol B-A* 119: 45–61
- FUCHS G, MATURA A (1976) Zur Geologie des Kristallins der südlichen Böhmischen Masse. *Jb Geol B-A* 119: 1–43
- GEBAUER D, FRIEDEL G (1994) A 1.38 Ga protolith age for the Dobra orthogneiss (Moldanubian Zone of the southern Bohemian Massif, NE-Austria): evidence from ion-microprobe (SHRIMP) dating of zircon. *J Czech Geol Soc* 39: 34–35
- GERDES A, FRIEDEL G, PARRISH RR, FINGER F (2003) High-resolution geochronology of Variscan granite emplacement the South Bohemian Batholith. *J Czech Geol Soc* 48: 53–54
- HANŽL P, MELICHAR R (1997) The Brno Massif: a section through the active continental margin or a composed terrane? *Krystalinikum* 23: 33–58
- HASALOVÁ P, JANOUŠEK V, SCHULMANN K, ŠTÍPSKÁ P, ERBAN V (2008) From orthogneiss to migmatite: geochemical assessment of the melt infiltration model in the Gföhl Unit (Moldanubian Zone, Bohemian Massif). *Lithos* 102: 508–537
- HENRY DJ, GUIDOTTI C V., THOMSON JA (2005) The Ti-saturation surface for low-to-medium pressure metapelitic biotites: implications for geothermometry and Ti-substitution mechanisms. *Amer Miner* 90: 316–328
- HÖCK V, MARSCHALLINGER M, TOPA D (1990) Granat–Biotit-Geothermometrie in Metapeliten der Moravischen Zone in Österreich. *Österr Beitr Met Geoph* 3: 149–167
- HÖGELSBERGER H (1989) Die Marmore und Kalksilikatgesteine der Bunten Serie – petrologische Untersuchungen und geologische Konsequenzen. *Jb Geol B-A* 132: 213–230
- HOLLAND TJB, BLUNDY J (1994) Non-ideal interactions in calcic amphiboles and their bearing on amphibole-plagioclase thermometry. *Contrib Mineral Petrol* 116: 433–447

- IMAI N, TERASHIMA S, ITOH S, ANDO A (1995) 1994 compilation values for GSJ reference samples, "Igneous rock series." *Geochem J* 29: 91–95
- IRVINE TN, BARAGAR WRA (1971) A guide to the chemical classification of the common volcanic rocks. *Canad J Earth Sci* 8: 523–548
- JANOUŠEK V, BOWES DR, ROGERS G, FARROW CM, JELÍNEK E (2000) Modelling diverse processes in the petrogenesis of a composite batholith: the Central Bohemian Pluton, Central European Hercynides. *J Petrol* 41: 511–543
- JANOUŠEK V, FARROW CM, ERBAN V (2006) Interpretation of whole-rock geochemical data in igneous geochemistry: introducing Geochemical Data Toolkit (GCDkit). *J Petrol* 47: 1255–1259
- JAWECKI C (1996) Fluid regime in the Austrian Moldanubian Zone as indicated by fluid inclusions. *Mineral Petrol* 58: 235–252
- JELÍNEK E, DUDEK A (1993) Geochemistry of subsurface Precambrian plutonic rocks from the Brunovistulian Complex in the Bohemian Massif, Czechoslovakia. *Precambr Res* 62: 103–125
- KALVODA J, BÁBEK O, FATKA O, LEICHMANN J, MELICHAR R, NEHYBA S, ŠPAČEK P (2008) Brunovistulian Terrane (Bohemian Massif, Central Europe) from late Proterozoic to late Paleozoic: a review. *Int J Earth Sci* 97: 497–518
- KOŠLER J, KONOPÁSEK J, SLÁMA J, VRÁNA S (2014) U–Pb zircon provenance of Moldanubian metasediments in the Bohemian Massif. *J Geol Soc, London* 171: 83–95
- KOSSMAT F (1927) Gliederung des varistischen Gebirgsbaus. *Abh Sächs Geol Landesamt* 1: 1–39
- KRÖNER U, ROMER RL (2013) Two plates – many subduction zones: the Variscan Orogeny reconsidered. *Gondwana Res* 24: 298–329
- LANARI P, WAGNER T, VIDAL O (2014) A thermodynamic model for di-trioctahedral chlorite from experimental and natural data in the system MgO–FeO–Al₂O₃–SiO₂–H₂O: applications to P–T sections and geothermometry. *Contrib Mineral Petrol* 167: 1–19
- LAURENT A, JANOUŠEK V, MAGNA T, SCHULMANN K, MÍKOVÁ J (2014) Petrogenesis and geochronology of a post-orogenic calc-alkaline magmatic association: the Žulová Pluton, Bohemian Massif. *J Geosci* 59: 415–440
- LARDEAUX JM, SCHULMANN K, FAURE M, JANOUŠEK V, LEXA O, SKRZYPEK E, EDEL JB, ŠTÍPSKÁ P (2014) The Moldanubian Zone in the French Massif Central, Vosges/Schwarzwald and Bohemian Massif revisited: differences and similarities. In: SCHULMANN K, MARTÍNEZ CATALÁN JR, LARDEAUX JM, JANOUŠEK V, OGGIANO G (eds) *The Variscan Orogeny: Extent, Timescale and the Formation of the European Crust*. Geological Society, London, Special Publications 405: pp 7–44
- LEAKE BE, WOOLLEY AR, ARPS CES, BIRCH WD, GILBERT MC, GRICE JD, HAWTHORNE FC, KATO A, KISCH HJ, KRIVOVICHEV VG, LINTHOUT K, LAIRD J, MANDARINO JA, MARESCH W V., NICKEL EH, ROCK NMS, SCHUMACHER JC, SMITH DC, STEPHENSON NCN, UNGARETTI L, WHITTACKER EJW, YOUNG G (1997) Nomenclature of amphiboles: report of the Subcommittee on Amphiboles of the International Mineralogical Association Commission on New Minerals and Mineral Names. *Mineral Mag* 61: 295–321
- LEICHMANN J, HÖCK V (2008) The Brno Batholith: an insight into the magmatic and metamorphic evolution of the Cadomian Brunovistulian Unit, eastern margin of the Bohemian Massif. *J Geosci* 53: 281–305
- LINDNER M (2016) Geochemische Charakterisierung von Spitzer und Dobra Gneis im Waldviertler Moldanubikum. Unpublished MSci Thesis, University of Salzburg, pp 1–107
- LINDNER M, FINGER F (2016) A geochemical study of the Dobra Gneiss in the Austrian part of the Moldanubian Zone. In: FINGER F, VERNER K, ŽÁK J, ZULAUF G (eds) *Proceedings of the 2nd Workshop on Orogenic Processes in the Bohemian Massif*. Czech Geological Survey, Prague, pp 30
- LINNEMANN U, ROMER RL, PIN C, ALEKSANDROWSKI P, BUŁA Z, GEISLER T, KACHLIK V, KRZEMIŃSKA E, MAZUR S, MOTUZA G, MURPHY JB, NANCE RD, PISAREVSKY SA, SCHULZ B, ULRICH J, WISZNIEWSKA J, ŽABA J, ZEH A (2008) The Precambrian. In: McCANN T (ed) *The Geology of Central Europe. Volume 1: Precambrian and Palaeozoic*. Geological Society, London, pp 21–102
- LINNER M (1992) Metamorphose der Paragneise in der Monotonen Serie (SE Moldanubikum). Unpublished MSci. Thesis, University of Vienna, pp 1–125
- LINNER M (1996) Metamorphism and partial melting of paragneisses of the Monotonous Group, SE Moldanubicum (Austria). *Mineral Petrol* 58: 215–234
- MATTE P, MALUSKI H, RAJLICH P, FRANKE W (1990) Terrane boundaries in the Bohemian Massif: result of large-scale Variscan shearing. *Tectonophysics* 177: 151–170
- MATURA A (1976) Hypothesen zum Bau und zur geologischen Geschichte des kristallinen Grundgebirges von Südwestmähren und dem niederösterreichischen Waldviertel. *Jb Geol B-A* 119: 63–75
- MATURA A (2003) Zur tektonischen Gliederung der variszischen Metamorphite im Waldviertel Niederösterreichs. *Jb Geol B-A* 143: 221–225
- MATZINGER M, FINGER F (2017) Bericht 2016 über geochemische und petrografische Untersuchungen an Orthogneisen aus dem Nationalpark Thayatal–Podyjí auf Blatt 9 Retz. *Jb Geol B-A* 157: 301–306
- MIELKE P, WINKLER HGF (1979) Eine bessere Berechnung der Mesonorm für granitische Gesteine. *Neu Jb Mineral Mh* 471–480
- MILLER CF, McDOWELL SM, MAPES RW (2003) Hot and cold granites: implications of zircon saturation temperatures and preservation of inheritance. *Geology* 31: 529–532

- NANCE RD, MURPHY JB, STRACHAN RA, KEPPIE JD, GUTIÉRREZ-ALONSO G, FERNÁNDEZ-SUÁREZ J, QUESADA C, LINNEMANN U, D'LEMOS RS, PISAREVSKY SA (2008) Neoproterozoic–early Palaeozoic tectonostratigraphy and palaeogeography of the peri-Gondwanan terranes: Amazonian v. West African connections. In: ENNIH N, LIÉGOIS JP (eds) *The Boundaries of the West African Craton*. Geological Society, London, Special Publications 297: pp 345–383
- O'BRIEN PJ, CARSWELL DA (1993) Tectonometamorphic evolution of the Bohemian Massif: evidence from high pressure metamorphic rocks. *Geol Rundsch* 82: 531–555
- O'BRIEN PJ, VRÁNA S (1995) Eclogites with a short-lived granulite-facies overprint in the Moldanubian Zone, Czech Republic – petrology, geochemistry and diffusion modeling of garnet zoning. *Geol Rundsch* 84: 473–488
- OTSEN MT (1984) The origin of brown hornblende in the Artfjället gabbro and dolerites. *Contrib Mineral Petrol* 86: 189–199
- PEARCE JA, HARRIS NBW, TINDLE AG (1984) Trace element distribution diagrams for the tectonic interpretation of granitic rocks. *J Petrol* 25: 956–983
- PECCERILLO A, TAYLOR SR (1976) Geochemistry of Eocene calc-alkaline volcanic rocks from the Kastamonu area, Northern Turkey. *Contrib Mineral Petrol* 58: 63–81
- PETRAKAKIS K (1997) Evolution of Moldanubian rocks in Austria: review and synthesis. *J Metamorph Geol* 15: 203–222
- RACEK M, ŠTÍPSKÁ P, PITRA P, SCHULMANN K, LEXA O (2006) Metamorphic record of burial and exhumation of orogenic lower and middle crust: a new tectonothermal model for the Drosendorf Window (Bohemian Massif, Austria). *Mineral Petrol* 86: 221–251
- RACEK M, LEXA O, SCHULMANN K, CORSINI M, ŠTÍPSKÁ P, MAIEROVÁ P (2017) Re-evaluation of polyphase kinematic and $^{40}\text{Ar}/^{39}\text{Ar}$ cooling history of Moldanubian hot nappe at the eastern margin of the Bohemian Massif. *Int J Earth Sci* 106: 397–420
- RENÉ M, FINGER F (2016) The Blaník Gneiss in the southern Bohemian Massif (Czech Republic): a rare rock composition among the early Palaeozoic granites of Variscan Central Europe. *Mineral Petrol* 110: 503–514
- RIEDER M, CAVAZZINI G, D'YAKONOV YS, FRANK-KAMENETSKII VA, GOTTAIDI G, GUGGENHEIM S, KOVAL P V, MUELLER G, NEIVA AMR, RADOSLOVICH EW, ROBERT JL, SASSI FP, TAKEDA H, WEISS Z, WONES DR (1999) Nomenclature of the micas. *Mineral Mag* 63: 267–279
- RUDNICK RL, GAO S (2003) Composition of the Continental Crust. In: HOLLAND HD, TUREKIAN KK (eds) *Treatise on Geochemistry 3, The Crust*. Elsevier, Amsterdam, pp 1–64
- SCHMIDT MW (1992) Amphibole composition in tonalite as a function of pressure: an experimental calibration of the Al-in-hornblende barometer. *Contrib Mineral Petrol* 110: 304–310
- SCHULMANN K, KRÖNER A, HEGNER E, WENDT I, KONOPÁSEK J, LEXA O, ŠTÍPSKÁ P (2005) Chronological constraints on the pre-orogenic history, burial and exhumation of deep-seated rocks along the eastern margin of the Variscan Orogen, Bohemian Massif, Czech Republic. *Amer J Sci* 305: 407–448
- SCOTT JM, KONRAD-SCHMOLKE M, O'BRIEN PJ, GÜNTHER C (2013) High-T, low-P formation of rare olivine-bearing symplectites in Variscan eclogite. *J Petrol* 54: 1375–1398
- SOEJONO I, JANOUŠEK V, ŽÁČKOVÁ E, SLÁMA J, KONOPÁSEK J, MACHEK M, HANŽL P (2017) Long-lasting Cadomian magmatic activity along an active northern Gondwana margin: U–Pb zircon and Sr–Nd isotopic evidence from the Brunovistulian Domain, eastern Bohemian Massif. *Int J Earth Sci* 106: 2109–2129
- SOUČEK J, JELÍNEK E, BOWES DR (1992) Geochemistry of gneisses of the eastern margin of the Bohemian Massif. In: KUKAL Z (ed) *Proceedings of the 1st International Conference on the Bohemian Massif*. Czech Geological Survey, Prague, pp 269–285
- STARIJAS MAYER B, KRENN E, FINGER F (2014) Microcrystals of Th-rich monazite (La) with a negative Ce anomaly in metadiorite and their role for documenting Cretaceous metamorphism in the Slavonian Mountains (Croatia). *Mineral Petrol* 108: 231–243
- ŠTELCL J, WEISS J (1986) *The Brno Massif*. University of J. E. Purkyně, Brno, pp 1–255 (in Czech)
- STRECKEISEN AL (1974) Classification and nomenclature of plutonic rocks. Recommendations of the IUGS Sub-commission on the Systematics of Igneous Rocks. *Geol Rundsch* 63: 773–786
- SUESS FE (1926) *Intrusionstektonik und Wandertektonik im variszischen Grundgebirge*. Gebrüder Bornträger, Berlin, pp 1–268
- SUN S -s., McDONOUGH WF (1989) Chemical and isotopic systematics of oceanic basalts: implications for mantle composition and processes. In: SAUNDERS AD, NORRY MJ (eds) *Magmatism in the Ocean Basins*. Geological Society, London, Special Publications 42: pp 313–345
- SVOJTKA M, BREITER K, DURIŠOVÁ J, ACKERMAN L, VESELOVSKÝ F, ŠMERDA J (2017) Geochemistry and U–Pb zircon ages of Derflice granodiorite from the Thaya (Dyje) Massif. *Geosci Res Rep* 50: 17–24 (in Czech)
- TAIT JA, BACHTADSE V, FRANKE W, SOFFEL H (1997) Geodynamic evolution of the European Variscan fold belt: palaeomagnetic and geological constraints. *Geol Rundsch* 86: 585–598
- TAYLOR SR (1968) Geochemistry of andesites. In: AHRENS LH (ed) *Origin and Distribution of the Elements*. Elsevier, Amsterdam, pp 559–583
- THIELE O (1984) Zum Deckenbau und Achsenplan des Moldanubikums der südlichen Böhmischen Masse (Österreich). *Jb Geol B-A* 126: 513–523

- VAN BREEMEN O, AFTALION M, BOWES DR, DUDEK A, MÍSAŘ Z, POVONDRA P, VRÁNA S (1982) Geochronological studies of the Bohemian Massif, Czechoslovakia, and their significance in the evolution of Central Europe. *Trans Roy Soc Edinb, Earth Sci* 73: 89–108
- VELLMER C (1992) Stoffbestand und Petrogenese von Granuliten und granitischen Gesteinen der südlichen Böhmischem Masse in Niederösterreich. Unpublished PhD Thesis, University of Göttingen, pp 1–111
- VENABLES WN, RIPLEY BD (2002) Modern Applied Statistics with S, 4th ed. Springer, New York, pp 1–498
- WALDMANN L (1938) Bericht über die geologischen Aufnahmen im Raume des Blattes "Horn (4555)" erstattet vom Privatdozenten Dr. Leo Waldmann. *Verh Geol B-A* 42–45
- WALDMANN L (1951) Das außeralpine Grundgebirge Österreichs. In: SCHAFFER FX (ed) *Geologie von Österreich*. Deuticke, Vienna, pp 1–105
- WALTER F, AUER C, BERNHARD F, BOJAR H, BRANDSTÄTTER F, GRÖBNER J, JAKELY D, KOLITSCH U, POSTL W, PRAYER A, SCHACHINGER T, SCHILLHAMMER H, SLAMA M, STECK C, WEISS J, ZEUG M (2017) Neue Mineralfunde aus Österreich LXVI. *Carinthia II* 207/127: 217–284
- WHITNEY DL, EVANS BW (2010) Abbreviations for names of rock-forming minerals. *Amer Miner* 95: 185–187
- WINCHESTER J, PACE TMR Network Team (2002) Palaeozoic amalgamation of Central Europe: new results from recent geological and geophysical investigations. *Tectonophysics* 360: 5–21
- XIE X, BYERLY GR, FERRELL JR RE (1997) IIb trioctahedral chlorite from the Barberton greenstone belt: crystal structure and rock composition constraints with implications to geothermometry. *Contrib Mineral Petrol* 126: 275–291
- ŽÁK J, VERNER K, JANOUŠEK V, HOLUB F V., KACHLÍK V, FINGER F, HAJNÁ J, TOMEK F, VONDROVIC L, TRUBAČ J (2014) A plate-kinematic model for the assembly of the Bohemian Massif constrained by structural relationships around granitoid plutons. In: SCHULMANN K, MARTÍNEZ CATALÁN JR, LARDEAUX JM, JANOUŠEK V, OGGIANO G (eds) *The Variscan Orogeny: Extent, Timescale and the Formation of the European Crust*. Geological Society, London, Special Publications 405: pp 169–196